TRITC-dextran (0.4 mg g^{-1} body weight) 4 h before killing. Whole blood was obtained by cardiac puncture at the time of sacrifice, and then the colonic tissues were examined whether the $EGFP^+$ engrafts were present. TRITC-dextran measurements were performed in duplicate on ARVO MX (PerkinElmer) with serial dilutions of TRITC-dextran in PBS used as a standard curve.

Supplementary Table.
Information on primers and reaction conditions for PCR

Gene	forward primer (5'-3')	reverse primer (5'-3')	annealing temp. (°C)	cycle number
Gapdh	CTGGCCAAGGTCATCCATGA	GCCATGAGGTCCACCACCCTG	60	19
Muc2	CCTTAGCCAAGGGCTCGGAA	GGCCCGAGAGTAGACCTTGG	60	25
CgA	CTGTCAGCCCTGAGTGTCTG	ATGGAAGTGGGAACTGGATG	58	31
CAII	AGCACAACGGACCAGAGAAC	CTGACAGTAATGGGCTCCCT	60	22
Cdh1	TGGACAGAGAAGACGCTGAG	ATCATCATCTGGTGGCAGCA	63	25
Lgr5	CTGACTTTGAATGGTGCCTCG	ATGTCCACTACCGCGATTAC	58	30
α-SMA	CGCTGTCAGGAACCCTGAGA	ATGAGGTAGTCGGTGAGATC	63	25

ORIGINAL ARTICLE

Association Study of 71 European Crohn's Disease Susceptibility Loci in a Japanese Population

Atsushi Hirano, MD,† Keiko Yamazaki, DVM, PhD,* Junji Umeno, MD, PhD,*† Kyota Ashikawa, MS,* Masayuki Aoki, MD, PhD,* Takayuki Matsumoto, MD, PhD,† Shotaro Nakamura, MD, PhD,† Toshiharu Ninomiya, MD, PhD,‡ Toshiyuki Matsui, MD, PhD,§ Fumihito Hirai, MD, PhD,§ Takaaki Kawaguchi, MD,‖ Masakazu Takazoe, MD,‖ Hiroki Tanaka, MD, PhD,¶ Satoshi Motoya, MD, PhD,¶ Yutaka Kiyohara, MD, PhD,‡ Takanari Kitazono, MD, PhD,† Yusuke Nakamura, MD, PhD,** Naoyuki Kamatani, MD, PhD,* and Michiaki Kubo, MD, PhD**

Background: A large-scale meta-analysis of a series of European genome-wide association studies revealed 71 susceptibility loci for Crohn's disease (CD). However, it is not clear whether these susceptibility loci are also shared with Japanese populations.

Methods: We genotyped 71 single-nucleotide polymorphisms (SNPs) comprising 1311 CD cases and 6585 controls of Japanese descent, and their associations with CD were evaluated using the Cochran–Armitage trend test. In addition, genotype–phenotype analyses were conducted on the SNPs showing associations with Japanese CD based on the Montreal classification.

Results: Twenty-seven SNPs showed at least nominal association ($P < 0.05$) and 11 of them remained significant even after Bonferroni correction ($P < 0.0007$). Despite high statistical power, we could not find any association in 17 loci. Moreover, SNPs in 9 loci were rare or absent in the Japanese population. Genetic variations involved in the innate immune system (*NOD2*, *ATG16L1*, and *IRGM*) showed no association with CD susceptibility in the Japanese population. Genotype–phenotype analyses showed that rs3810936, a marker of *TNFSF15*, correlated with severe CD phenotypes.

Conclusions: Our study suggests that there is a differential genetic background of CD susceptibility between Japanese and European populations.

(Inflamm Bowel Dis 2013;19:526–533)

Key Words: Crohn's disease, Japanese, innate immune system, *TNFSF15*

Crohn's disease (CD) is one of the major subtypes of inflammatory bowel disease. It is hypothesized that CD is a multifactorial disease caused by multiple environmental and genetic factors. To date, several genome-wide association (GWA) studies of CD have been conducted, and recently a large-scale meta-analysis of GWA studies has identified 71 CD susceptibility loci in European populations.[1] This knowledge has brought several insights into the pathogenesis of CD. The importance of the innate and adaptive immune responses was particularly highlighted. In the innate arm of the immune system, it has been shown that *NOD2*, which encodes an intracellular sensor of bacterial muramyl dipeptide, and 2 autophagy-related genes (*ATG16L1* and *IRGM*) are strongly associated with CD.[1–4] In the adaptive arm of the immune system, GWA studies have identified genes related to the interleukin (IL)-23–T_H17 pathway, including *IL23R*, *IL12B*, *JAK2*, *STAT3*, *CCR6*, and *TNFSF15*.[1,2,5,6]

So far, the majority of GWA studies on CD have been performed in European populations. Although it has been reported that several CD susceptibility loci identified in European GWA studies are not associated with CD in Japanese populations,[7–11] it has not been thoroughly investigated whether the remaining European CD susceptibility loci are shared with other ethnicities. To the best of our knowledge, only a few genetic studies have been performed in Asian populations,[6–13] and it is unclear which genomic regions contribute to the genetic susceptibility of the Asians to CD. Therefore, we conducted a case–control association study to investigate the association of 71 European CD susceptibility loci in a Japanese population.

In addition, a number of genotype–phenotype analyses have been conducted on the CD susceptibility loci in European

Supplemental digital content is available for this article. Direct URL citations appear in the printed text and are provided in the HTML and PDF versions of this article on the journal's Web site (www.ibdjournal.org).

Received for publication July 26, 2012; Accepted August 4, 2012.

From the *Laboratory for Genotyping Development, Center for Genomic Medicine, RIKEN Yokohama Institute, Yokohama, Japan; †Department of Medicine and Department of Clinical Science, ‡Department of Environmental Medicine, Graduate School of Medical Sciences, Kyushu University, Fukuoka, Japan; §Department of Gastroenterology, Fukuoka University Chikushi Hospital, Fukuoka, Japan; ‖Department of Medicine, Division of Gastroenterology, Social Insurance Chuo General Hospital, Tokyo, Japan; ¶Department of Gastroenterology, Sapporo-Kosei General Hospital, Sapporo, Japan; and **Human Genome Center, Institute of Medical Science, the University of Tokyo, Tokyo, Japan.

The authors have no conflicts of interest to disclose.

This work was conducted as a part of the BioBank Japan Project and supported by a Grant-in-Aid for Young Scientists (A) (22689025) from the Ministry of Education, Culture, Sports, Sciences and Technology of the Japanese government.

Reprints: Michiaki Kubo, MD, PhD, Laboratory for Genotyping Development, Center for Genomic Medicine, RIKEN Yokohama Institute, 1-7-22, Suehiro-cho, Tsurumi, Yokohama, Kanagawa 230-0045, Japan (e-mail: mkubo@src.riken.jp).

DOI 10.1097/MIB.0b013e31828075e7

Published online 6 February 2013.

CD populations, and *NOD2*, the strongest CD susceptibility gene in Europeans, is shown to be associated with CD severity such as early onset[14,15] and complicated behavior.[15–17] However, in the Japanese CD population, there is little information about the relationship between CD susceptibility loci and disease severity. We thus performed genotype–phenotype analyses on the associated loci in the Japanese CD population.

MATERIALS AND METHODS

Patients and Controls

A total of 1311 CD cases and 6585 controls were enrolled in this study. CD cases were collected at the Kyushu University Hospital (n = 160), its 16 affiliated hospitals (n = 447), Social Insurance Central General Hospital (n = 526), and Sapporo Kosei General Hospital (n = 178). All CD cases were diagnosed by clinical, radiological, endoscopic, and histological findings according to the Lennard–Jones criteria.[18] Clinical information of patients with CD was assessed at the time of sample collection, and phenotypes were categorized using Montreal classification.[19] Control subjects consisted of 3196 participants of the Hisayama study between 2002 and 2003[20] and 3389 samples selected from the BioBank Japan Project. This project (http://biobankjp.org) was started in 2003 to collect genomic DNA, serum, and clinical information of approximately 200,000 patients diagnosed with any of the 47 diseases by a collaborative network of 66 hospitals in Japan.[21] All participants were of Japanese descent.

Informed consent was obtained for all cases and controls before the study participation. This study was approved by the ethics committees of both RIKEN Yokohama Institute and Kyushu University.

Single-Nucleotide Polymorphism Selection for Case–Control Analysis and Genotyping

We selected 71 single-nucleotide polymorphisms (SNPs) that were reported to tag CD susceptibility loci in European populations. The SNPs were those imputed from data taken from 6 European GWA studies using HapMap3 reference data, and that were found to be significantly associated with CD in the meta-analysis of these GWAS followed by a replication study.[1] In this study, all SNPs were genotyped using the Invader assay (Third Wave Technologies, Madison, WI).[22] The overall call rate was 99.0%.

Statistical Analysis

Case–control association was analyzed using the Cochran–Armitage trend test, since χ^2 statistics from the 2×2 allelic table is inappropriate if the Hardy–Weinberg equilibrium does not hold in the combined case–control population.[23] Assessments of departure from the Hardy–Weinberg equilibrium in control samples were performed using χ^2 test. We considered a $P < 0.05$ as nominal association and a $P < 0.0007$ (0.05/71) as significant association in this study. To facilitate determination of risk direction, we calculated the odds ratios (ORs) and 95% confidence intervals of each SNP according to the risk alleles, as described in the original study.[1] Statistical power was estimated by the Genetic Power Calculator[24] using both ORs described in the original article[1] and allele frequencies from HapMap JPT data. Linkage disequilibrium coefficients (r^2) were calculated with the Haploview v4.2 [25] using HapMap JPT and CEU data. Genotype–phenotype analyses were conducted on those SNPs that showed significant association with CD in the present study. Primarily, CD cases were stratified on the basis of the Montreal classification for age at diagnosis, disease location, and disease behavior. In addition, CD cases were further sorted into 2 groups with respect to each category as follows: A1 (16 years or younger) versus A2 + A3 (17 years or older) for age at diagnosis, L1 (±L4) + L2 (±L4) (mainly localized in either ileum or colon) versus L3 (±L4) (spread in both ileum and colon) for disease location, and B1 (nonstricturing and nonpenetrating behavior) versus B2 + B3 (stricturing or penetrating behavior) for disease behavior. In these 3 categories, we performed case–case comparisons using the Cochran–Armitage trend test. Phenotypic groups of A1 (diagnosed at 16 years or younger), L3 (±L4) (spread in both ileum and colon), and B2 + B3 (stricturing or penetrating behavior) were regarded as severe phenotypes, whereas complementary phenotypic groups were regarded as reference phenotypes. For general statistical analysis, we used the R statistical environment (Version 2.13.0).

RESULTS

Clinical Characteristics

A total of 1311 CD cases and 6585 controls were examined. The clinical characteristics of the study population are summarized in Table 1. The proportion of males was higher in CD cases (70.2%) than in the controls (49.4%), and the mean age at sampling was lower in CD cases (36.0 years) than in the controls (55.0 years). The phenotype information was not available in almost 14% of the cases, and the remaining cases were stratified on the basis of the Montreal classification.

Case Control Analysis for 71 SNPs in a Japanese Population

No marker showed significant deviation from the Hardy–Weinberg equilibrium after Bonferroni correction. Twenty-seven SNPs showed at least nominal association with CD ($P < 0.05$), and 11 of them showed significant association even after Bonferroni correction ($P < 0.05/71 = 0.0007$) (Table 2). These significant loci included genes encoding *TNFSF15*, *NKX2-3*, *ICOSLG*, *HLA*, *IL12B*, *REL*, *VAMP3*, and *PLCL1*. We inferred that these loci might be common CD susceptibility loci for both Japanese and European populations.

On the other hand, 17 SNPs did not show any association with CD despite the high statistical power of our study (Table 3). Moreover, we found that the minor alleles of an additional 9 SNPs were rare (<1%) or absent in both cases and controls (Table 4), which contrasts with that observed in the GWA meta-analysis in European populations.[1] With regard to the remaining 18 SNPs, no conclusion could be drawn because the statistical power of this

TABLE 1. Clinical Characteristics of Patients with CD and Controls

	Cases (N = 1311)	Controls (N = 6585)
Sex		
Male/female	920 (70.2%)/ 390 (29.8%)	3227 (49.4%)/ 3302 (50.6%)
Not available	1	56
Age at sampling (yr)		
Mean (±SD)	36.0 (±11.6)	55.0 (±15.2)
Age at diagnosis[b]		
16 years or younger (A1)	160 (14.1%)	
Between 17 and 40 yr (A2)	884 (78.0%)	
Over 40 yr (A3)	89 (7.9%)	
Not available	178	
Disease location[b]		
Terminal ileum (L1) ± L4[a]	445 (39.3%)	
Colon (L2) ± L4[a]	172 (15.2%)	
Ileocolon (L3) ± L4[a]	514 (45.5%)	
Not available	180	
Disease behavior[bc]		
Nonstricturing, nonpenetrating (B1)	297 (26.3%)	
Stricturing (B2)	487 (43.1%)	
Penetrating (B3)	345 (30.6%)	
Not available	182	

[a]L4:upper gastrointestine.
[b]Phenotypes were categorized using Montreal classification.
[c]Perianal disease was not evaluated because clinical information was inadequate.

study was too low (see Table, Supplemental Digital Content 1, http://links.lww.com/IBD/A74).

To highlight the genetic differences in the CD susceptibility loci between Japanese and European populations, we compared the result of our data with the top 10 CD-associated SNPs in the European meta-analysis.[1] In these 10 SNPs, only a marker of *ZNF365* (rs10761659) was associated with a similar genetic risk in both populations. Out of the other 9 SNPs, the 5 markers of *MUC19/LRRK2* (rs11564258), *IRGM* (rs7714584), *ATG16L1* (rs3792109), *PTGER4* (rs11742570), and *PTPN2* (rs1893217) had no significant genetic effect in the Japanese population. Moreover, minor alleles of 4 markers of *IL23R* (rs11209026), *NOD2* (rs2076756), *PTPN22* (rs2476601), and *SLC22A4/SLC22A5/IRF1/IL3* (rs12521868) loci were very rare or absent in the Japanese population. These results reflect the genetic diversity at the single SNP level and suggest that there might be differences in the genetic background of CD between Europeans and Asians.

Association Between Genotypes and CD Severity

We conducted genotype–phenotype analyses on the 11 markers that showed significant association in this study. The marker SNP of *TNFSF15* (rs3810936), which was strongly associated with CD in the Japanese population, was shown to be associated with all 3 phenotype categories (Table 5). The CD risk allele C of rs3810936 was associated with the diagnosis at the age of 16 or younger (OR = 1.42), ileocolonic location (OR = 1.34), and stricturing or penetrating behavior (OR = 1.34). These phenotypes represent early onset, extensive lesion, and complicated behavior, respectively. Therefore, the result suggests that the variation in *TNFSF15* is associated with CD severity. The other 10 markers did not show any subphenotype association. Our study had sufficient power (≥80%) to detect the subphenotype association in almost all analyses, assuming an OR of 1.7 or more (data not shown).

DISCUSSION

We examined 71 European CD susceptibility loci in a Japanese population and found that at least 11 susceptibility loci are common to both European and Japanese populations. Among these 11 loci, 3 loci (*TNFSF15*, *NKX2-3*, and *IL12B*) were already reported to be associated with Japanese CD,[6,12] but, to the best of our knowledge, this study is the first to show the significant association of the additional 8 loci in the Japanese population. On the other hand, our study revealed that 17 loci did not show any association with CD in the Japanese population, despite high statistical power.

In interpreting our results, it is important to note that we tested the SNPs reported in the European GWA study.[1] Although some of these SNPs were the same as functional variants, the remaining SNPs were markers tagging functional variants in European populations. To evaluate the association of CD susceptibility loci properly, we should consider whether the tested SNPs tagged the functional variants in the Japanese subjects. In this study, tested SNPs in *TNFSF15* locus and *NKX2-3* locus are highly linked to the functional variants,[26,27] and these SNPs showed significant association in the Japanese population (Table 2). Although the tested SNPs in *ATG16L1* locus, *IRGM* locus, *PTPN2* locus, and *MST1* locus are also highly linked to the functional variants[28–32] in both European and Japanese populations, these SNPs showed no association in the Japanese population despite the high statistical power. This result indicates that these functional variants are indeed unlikely important in the Japanese population (Table 3).

Although it is not clear why the SNPs in *ATG16L1* and *IRGM* loci tagging functional variants did not show any association with CD, there may be several reasons for this. First, the differences in the environmental factors among populations may alter the effect of these variations. For instance, a previous study of twins indicated that differences in microbial compositions are correlated with the disease phenotype in monozygotic twins with identical genetic backgrounds.[33] If such differences in microbial composition exist at the population level, they may modulate the effect of the variants in the *ATG16L1* and *IRGM* loci in Japanese versus European

TABLE 2. SNPs Showing At Least Nominal Association with CD

Tested SNPs	Functional Variants[a]	r^2[b] JPT	r^2[b] CEU	Risk Allele[c]	RAF Cases	RAF Controls	*P*	OR (95% CI)[d]	Candidate Genes[e]
rs3810936	rs6478109	0.77	0.72	C	0.75	0.61	2.67×10^{-38} [g]	1.87 (1.70–2.06)	*TNFSF15, TNFSF8*
rs4409764	rs11190140	0.97	0.96	T	0.48	0.41	1.43×10^{-9} [g]	1.29 (1.19–1.41)	*NKX2-3*
rs2838519	—	—	—	G	0.66	0.61	2.51×10^{-7} [g]	1.26 (1.16–1.38)	*ICOSLG*
rs1799964	—	—	—	C	0.20	0.17	2.23×10^{-6} [g]	1.29 (1.16–1.43)	*LTA, HLA-DQA2, TNF, LST1, LTB*
rs6556412	—	—	—	A	0.52	0.47	9.01×10^{-6} [g]	1.21 (1.11–1.32)	*IL12B*
rs1736020	—	—	—	C	0.86	0.83	6.10×10^{-5} [g]	1.28 (1.14–1.44)	
rs10181042	—	—	—	T	0.06	0.05	6.63×10^{-5} [g]	1.44 (1.20–1.71)	*C2orf74, REL*
rs2797685	—	—	—	A	0.50	0.46	1.48×10^{-4} [g]	1.18 (1.08–1.28)	*VAMP3*
rs3764147	—	—	—	G	0.39	0.35	2.01×10^{-4} [g]	1.18 (1.08–1.28)	*C13orf31*
rs6738825	—	—	—	A	0.75	0.72	5.73×10^{-4} [g]	1.18 (1.08–1.30)	*PLCL1*
rs7702331	—	—	—	A	0.84	0.81	6.79×10^{-4} [g]	1.21 (1.08–1.36)	
rs780093	—	—	—	T	0.59	0.55	7.57×10^{-4} [f]	1.16 (1.06–1.26)	*GCKR*
rs151181	—	—	—	G	0.15	0.13	1.58×10^{-3} [f]	1.21 (1.07–1.36)	*IL27, SH2B1, EIF3C, LAT, CD19*
rs8005161	—	—	—	T	0.20	0.18	1.79×10^{-3} [f]	1.18 (1.06–1.31)	*GALC, GPR65*
rs10761659	rs7076156	0.05	0.21	G	0.73	0.70	1.84×10^{-3} [f]	1.16 (1.06–1.28)	*ZNF365*
rs694739	—	—	—	A	0.81	0.79	6.97×10^{-3} [f]	1.16 (1.04–1.29)	*PRDX5, ESRRA*
rs1250550	—	—	—	G	0.56	0.53	7.70×10^{-3} [f]	1.12 (1.03–1.22)	*ZMIZ1*
rs4809330	—	—	—	G	0.41	0.38	8.29×10^{-3} [f]	1.12 (1.03–1.22)	*RTEL1, TNFRSF6B, SLC2A4RG*
rs12242110	—	—	—	G	0.27	0.25	0.0108 [f]	1.13 (1.03–1.24)	*CREM*
rs713875	—	—	—	C	0.26	0.24	0.0155 [f]	1.13 (1.02–1.24)	*MTMR3*
rs11871801	—	—	—	A	0.87	0.85	0.0157[f]	1.16 (1.03–1.32)	*MLX, STAT3*
rs4656940	—	—	—	A	0.62	0.60	0.0174 [f]	1.11 (1.02–1.21)	*CD244, ITLN1*
rs181359	—	—	—	T	0.50	0.48	0.0180 [f]	1.11 (1.02–1.20)	*YDJC*
rs1819658	—	—	—	C	0.61	0.58	0.0238 [f]	1.10 (1.01–1.20)	*UBE2D1*
rs415890	—	—	—	C	0.52	0.49	0.0247 [f]	1.10 (1.01–1.20)	*CCR6*
rs17309827	—	—	—	T	0.57	0.55	0.0343 [f]	1.10 (1.01–1.19)	
rs7517810	—	—	—	T	0.92	0.91	0.0366 [f]	1.18 (1.01–1.38)	*TNFSF18, TNFSF4, FASLG*

[a]These variants have been reported as functional variants in the previous studies.
[b]r^2 between a tested SNP and a functional variant was calculated with Haploview using HapMap JPT and CEU database.
[c]Risk alleles are concordant with those of the original paper.[1]
[d]All associations are in the same direction, as described in the original paper.[1]
[e]Candidate genes are those presented in the original paper.[1]
[f]SNPs showed nominal association with CD ($0.0007 \leq P < 0.05$).
[g]SNPs showed significant association with CD even after Bonferroni correction ($P < 0.0007$).
RAF, risk allele frequency; CI, confidence interval.

TABLE 3. SNPs Showing No Association with CD Despite High Statistical Power

Tested SNPs	Functional Variants[a]	r^{2b}		Risk Allele[c]	RAF		P	OR (95% CI)	Candidate Genes[d]	Statistical Power[e] (%)
		JPT	CEU		Cases	Controls				
rs3180018	—	—	—	A	0.75	0.74	0.191	1.07 (0.97–1.17)	SCAMP3, MUC1	68.1
rs3197999	rs3197999	1	1	A	0.05	0.04	0.232	1.13 (0.92–1.38)	MST1, GPX1, BSN	78.4
rs7927997	—	—	—	T	0.14	0.14	0.636	1.03 (0.91–1.16)	C11orf30	79.7
rs2872507	—	—	—	A	0.26	0.26	0.669	1.02 (0.93–1.12)	*GSMDL, ZPBP2, ORMDL3, IKZF3*	82.6
rs1456896	—	—	—	T	0.52	0.51	0.243	1.05 (0.97–1.14)	*IKZF1, ZPBP, FIGNL1*	85.5
rs6908425	—	—	—	C	0.80	0.79	0.426	1.04 (0.94–1.16)	*CDKAL1*	86.1
rs1893217	rs1893217	1	1	G	0.12	0.12	0.520	0.96 (0.84–1.09)	*PTPN2*	91.8
rs740495	—	—	—	G	0.43	0.44	0.775	0.99 (0.91–1.08)	*GPX4, SBNO2*	93.3
rs4077515	—	—	—	T	0.32	0.33	0.197	0.94 (0.86–1.03)	*CARD9, SNAPC4*	94.4
rs4871611	—	—	—	A	0.38	0.38	0.958	1.00 (0.92–1.09)		95.5
rs10758669	—	—	—	C	0.37	0.36	0.201	1.06 (0.97–1.15)	*JAK2*	96.9
rs2058660	—	—	—	G	0.46	0.45	0.117	1.07 (0.98–1.16)	*IL18RAP, IL12RL2, IL18R1, IL1RL1*	98.2
rs11564258	rs3761863	0.01	0.04	A	0.03	0.03	0.898	1.02 (0.81–1.28)	*MUC19, LRRK2*	98.7
rs3091315	—	—	—	A	0.36	0.36	0.624	0.98 (0.90–1.07)	*CCL2, CCL7*	98.7
rs11742570	—	—	—	C	0.16	0.16	0.312	1.06 (0.95–1.19)	*PTGER4*	99.9
rs7714584	20 kb deletion[f]	1	1	G	0.40	0.38	0.060	1.09 (1.00–1.18)	*IRGM*	100.0
	rs10065172	1	1							
rs3792109	rs2241880	1	0.97	A	0.24	0.23	0.418	1.04 (0.94–1.15)	*ATG16L1*	100.0

[a]These variants have been reported as functional variants in the previous studies.
[b]r^2 between a tested SNP and a functional variant was calculated with Haploview using HapMap JPT and CEU database.
[c]Risk alleles are concordant with those of the original paper.[1]
[d]Candidate genes are those presented in the original paper.[1]
[e]Statistical power was estimated using both ORs described in the original paper[1] and allele frequencies from HapMap database.
[f]This variant is 20 kb deletion that maps 1.6 kb upstream of *IRGM*.
RAF, risk allele frequency; CI, confidence interval.

TABLE 4. SNPs Whose Minor Alleles Were Very Rare (<1%) or Absent in a Japanese Population

Tested SNPs	Functional Variants[a]	r^{2b}		Risk Allele[c]	RAF		*P*	OR (95% CI)	Candidate Genes[d]
		JPT	CEU		Cases	Controls			
rs10495903	—	—	—	T	0.0053	0.0060	0.722	0.90 (0.51–1.59)	*THADA*
rs2476601	rs2476601	1	1	G	0.9996	0.9999	0.204	0.20 (0.01–3.18)	*PTPN22*
rs2076756	rs2066844	NA	NA	G	0	0.0014	0.052	NA	*NOD2*
	rs2066845	NA	NA						
	rs2066847	NA	NA						
rs6568421	—	—	—	G	0	0.0003	0.372	NA	*PRDM1*
rs12521868	rs1050152	—[e]	0.93	T	0.0008	0.0004	0.395	2.01 (0.39–10.37)	*SLC22A4, SLC22A5, IRF1, IL3*
	rs2631367	—[e]	NA						
rs281379	rs601338	—[e]	0.75	A	0	0.0002	0.439	NA	*FUT2, RASIP1*
rs11209026	rs11209026	1	1	G	1	1	NA	NA	*IL23R*
rs12720356	—	—	—	G	0	0	NA	NA	*TYK2, ICAM1, ICAM3*
rs7423615	—	—	—	T	0	0	NA	NA	*SP140*

[a]Reported as functional variants in the previous studies.
[b]r^2 between a tested SNP and a functional variant was calculated with Haploview using HapMap JPT and CEU database.
[c]Risk alleles are concordant with those of the original paper.[1]
[d]Candidate genes are those presented in the original paper.[1]
[e]Rs12521868, rs1050152, rs2631367, and rs281379 are monomorphic in HapMap JPT database.
RAF, risk allele frequency; CI, confidence interval; NA, not available.

populations. Second, although functional interactions between *ATG16L1* and *NOD2* in the intracellular antibacterial response have been reported,[34,35] 3 coding variants of *NOD2*, which were strongly associated with CD in European populations, were not polymorphic in Asian populations.[7,8,13] If *NOD2* variants have an impact on the contribution of the *ATG16L1* variant to pathogenesis, the absence of *NOD2* variants may weaken the effect of the *ATG16L1* variant in the Japanese population. Third, it was revealed that a synonymous variant in *IRGM* (rs10065172) alters a microRNA-binding site and causes deregulation of IRGM-dependent xenophagy.[30] If the microRNA profile of Japanese individuals is different from that of Europeans, the effect of the microRNA-binding site variant may be less penetrant in the Japanese population.

In addition to *ATG16L1* and *IRGM*, *NOD2* is involved in the innate immune system. A tested SNP of *NOD2* locus, which is

TABLE 5. Genotype–Phenotype Association in *TNFSF15* (rs3810936)

Phenotype[a]	Genotype			RAF	*P*[b]	OR (95% CI)[c]
	CC	CT	TT			
Age at diagnosis						
A1 (16 yr or younger)	104	47	8	0.80	0.0180	1.42 (1.06–1.91)
A2 + A3 (17 yr or older)	528	381	62	0.74		
Disease location						
L3 (±L4) (ileocolon)	311	178	24	0.78	0.0025	1.34 (1.11–1.63)
L1 (±L4) + L2 (±L4) (ileum or colon)	319	249	44	0.72		
Disease behavior						
B2 + B3 (stricturing or penetrating)	479	310	42	0.76	0.0060	1.34 (1.09–1.65)
B1 (nonstricturing and nonpenetrating)	150	118	28	0.71		

[a]Phenotypes were categorized using Montreal classification.
[b]*P* values were calculated using the Cochran–Armitage trend test.
[c]ORs were calculated using phenotypic subgroups described in lower rows as references.
RAF, risk allele frequency; CI, confidence interval.

a marker tagging functional variants in the European populations, did not show any association in this study because the minor allele of the tested SNP was very rare in the Japanese subjects. Furthermore, it has been reported that 3 known functional variants of *NOD2* locus are absent in Japanese populations.[7,8] These results suggest that genetic variations involved in the innate immune system may not have crucial roles in CD susceptibility in the Japanese population. Meanwhile, our study showed that several genes involved in the IL-23–T_H17 pathway (*TNFSF15*, *IL12B*, *STAT3*, and *CCR6*) are associated with CD susceptibility in the Japanese population. These findings underscore the importance of the adaptive immune system in CD pathogenesis across various populations.

Although it has been reported that *NOD2* is correlated with CD severity such as early onset[14,15] and complicated behavior[15–17] in European CD populations, no loci correlated with CD severity has been identified in the Japanese CD population. To elucidate the loci correlated with CD severity, we conducted genotype–phenotype analyses on 11 common susceptibility loci for European and Japanese populations and identified that a marker of *TNFSF15* (rs3810936) might be related to severe phenotypes such as early age of diagnosis, ileocolonic location, and complicated behavior. However, previous genotype–phenotype analyses of the *TNFSF15* locus did not find any significant association in either European[36,37] or Korean population.[38] One reason for this conflicting result might be the smaller sample sizes in the previous studies.[36–38] The association between variations in *TNFSF15* and CD phenotypes should be confirmed by additional studies in the future.

There are some limitations in this study. We used ORs derived from European populations to calculate statistical power in this study. However, this approach might be imperfect because ORs are highly correlated with allele frequencies within a particular population. When we calculated the statistical power in this study, the lowest effect sizes detected with 80% power were 1.64, 1.29, 1.21, and 1.16 for the risk allele frequencies of 0.01, 0.05, 0.1, and 0.2, respectively. Therefore, further studies with larger sample size will be required to clarify the associations of established CD susceptibility loci with low allele frequency in Japanese populations.

In conclusion, we assessed whether 71 CD susceptibility loci identified in the European GWA studies were associated with Japanese CD. Our study identified at least 11 susceptibility loci that are common to both European and Japanese populations. We also revealed distinct ethnic differences in the genetic background of CD susceptibility, especially in the innate immune system–related loci. Further studies will be needed to clarify the shared or differential genetic background of CD susceptibility between European and Asian populations.

ACKNOWLEDGMENTS

We thank the patients with Crohn's disease and residents of Hisayama for their participation, all members of the Division of Health and Welfare of Hisayama for their cooperation, and many members of the Hisayama study for assistance. We thank all the patients who participated in BioBank Japan project, all members of BioBank Japan, and the members of the Center for Genomic Medicine, RIKEN, for their contribution to the completion of our study. For collecting clinical samples, we thank K. Aoyagi, H. Koga, M. Esaki, S. Yada, T. Moriyama, K. Asano, Y. Sakai, H. Suekane, K. Hirakawa, K. Hizawa, T. Tabata, H. Yamagata, S. Osamura, M. Seo, K. Saijo, and J. Nakashima.

REFERENCES

1. Franke A, McGovern DP, Barrett JC, et al. Genome-wide meta-analysis increases to 71 the number of confirmed Crohn's disease susceptibility loci. *Nat Genet.* 2010;42:1118–1125.
2. Duerr RH, Taylor KD, Brant SR, et al. A genome-wide association study identifies IL23R as an inflammatory bowel disease gene. *Science.* 2006; 314:1461–1463.
3. Hampe J, Franke A, Rosenstiel P, et al. A genome-wide association scan of nonsynonymous SNPs identifies a susceptibility variant for Crohn disease in ATG16L1. *Nat Genet.* 2007;39:207–211.
4. The Wellcome Trust Case Control Consortium. Association scan of 14,500 nonsynonymous SNPs in four diseases identifies autoimmunity variants. *Nat Genet.* 2007;39:1329–1337.
5. Barrett JC, Hansoul S, Nicolae DL, et al. Genome-wide association defines more than 30 distinct susceptibility loci for Crohn's disease. *Nat Genet.* 2008;40:955–962.
6. Yamazaki K, McGovern D, Ragoussis J, et al. Single nucleotide polymorphisms in TNFSF15 confer susceptibility to Crohn's disease. *Hum Mol Genet.* 2005;14:3499–3506.
7. Yamazaki K, Takazoe M, Tanaka T, et al. Absence of mutation in the NOD2/CARD15 gene among 483 Japanese patients with Crohn's disease. *J Hum Genet.* 2002;47:469–472.
8. Inoue N, Tamura K, Kinouchi Y, et al. Lack of common NOD2 variants in Japanese patients with Crohn's disease. *Gastroenterology.* 2002;123:86–91.
9. Yamazaki K, Onouchi Y, Takazoe M, et al. Association analysis of genetic variants in IL23R, ATG16L1 and 5p13.1 loci with Crohn's disease in Japanese patients. *J Hum Genet.* 2007;52:575–583.
10. Yamazaki K, Takazoe M, Tanaka T, et al. Association analysis of SLC22A4, SLC22A5 and DLG5 in Japanese patients with Crohn disease. *J Hum Genet.* 2004;49:664–668.
11. Prescott NJ, Dominy KM, Kubo M, et al. Independent and population-specific association of risk variants at the IRGM locus with Crohn's disease. *Hum Mol Genet.* 2010;19:1828–1839.
12. Yamazaki K, Takahashi A, Takazoe M, et al. Positive association of genetic variants in the upstream region of NKX2-3 with Crohn's disease in Japanese patients. *Gut.* 2009;58:228–232.
13. Thia KT, Loftus EV, Sandborn WJ, et al. An update on the epidemiology of inflammatory bowel disease in Asia. *Am J Gatroenterol.* 2008;103: 3167–3182.
14. Ahmad T, Armuzzi A, Bunce M, et al. The molecular classification of the clinical manifestations of Crohn's disease. *Gastroenterology.* 2002;122: 854–866.
15. Gearry RB, Roberts RL, Burt MJ, et al. Effect of inflammatory bowel disease classification changes on NOD2 genotype-phenotype associations in a population-based cohort. *Inflamm Bowel Dis.* 2007;13:1220–1227.
16. Economou M, Trikalinos TA, Loizou KT, et al. Differential effects of NOD2 variants on Crohn's disease risk and phenotype in diverse populations: a metaanalysis. *Am J Gastroenterol.* 2004;99:2393–2404.
17. Adler J, Rangwalla SC, Dwamena BA, et al. The prognostic power of the NOD2 genotype for complicated Crohn's disease: a meta-analysis. *Am J Gastroenterol.* 2011;106:699–712.
18. Lennard-Jones JE. Classification of inflammatory bowel disease. *Scand J Gastroenterol Suppl.* 1989;170:2–6.
19. Silverberg MS, Satsangi J, Ahmad T, et al. Toward an integrated clinical, molecular and serological classification of inflammatory bowel disease: Report of a Working Party of the 2005 Montreal World Congress of Gastroenterology. *Can J Gastroenterol.* 2005;19(suppl A):5–36.

20. Kubo M, Hata J, Ninomiya T, et al. A nonsynonymous SNP in PRKCH (protein kinase C eta) increases the risk of cerebral infarction. *Nat Genet.* 2007;39:212–217.
21. Nakamura Y. The Biobank Japan Project. *Clin Adv Hematol Oncol.* 2007; 5:696–7.
22. Ohnishi Y, Tanaka T, Ozaki K, et al. A high-throughput SNP typing system for genome-wide association studies. *J Hum Genet.* 2001;46: 471–477.
23. Sasieni PD. From genotypes to genes: doubling the sample size. *Biometrics.* 1997;53:1253–1261.
24. Purcell S, Cherny SS, Sham PC. Genetic Power Calculator: design of linkage and association genetic mapping studies of complex traits. *Bioinformatics.* 2003;19:149–150.
25. Barrett JC, Fry B, Maller J, et al. Haploview: analysis and visualization of LD and haplotype maps. *Bioinformatics.* 2005;21:263–265.
26. Kakuta Y, Ueki N, Kinouchi Y, et al. TNFSF15 transcripts from risk haplotype for Crohn's disease are overexpressed in stimulated T cells. *Hum Mol Genet.* 2009;18:1089–1098.
27. John G, Hegarty JP, Yu W, et al. NKX2-3 variant rs11190140 is associated with IBD and alters binding of NFAT. *Mol Genet Metab.* 2011;104: 174–179.
28. Kuballa P, Huett A, Rioux JD, et al. Impaired autophagy of an intracellular pathogen induced by a Crohn's disease associated ATG16L1 variant. *PLoS One.* 2008;3:e3391.
29. McCarroll SA, Huett A, Kuballa P, et al. Deletion polymorphism upstream of IRGM associated with altered IRGM expression and Crohn's disease. *Nat Genet.* 2008;40:1107–1112.
30. Brest P, Lapaquette P, Souidi M, et al. A synonymous variant in IRGM alters a binding site for miR-196 and causes deregulation of IRGM-dependent xenophagy in Crohn's disease. *Nat Genet.* 2011;43:242–245.
31. Scharl M, Mwinyi J, Fischbeck A, et al. Crohn's disease-associated polymorphism within the PTPN2 gene affects muramyl-dipeptide-induced cytokine secretion and autophagy. *Inflamm Bowel Dis.* 2012; 18:900–912.
32. Gorlatova N, Chao K, Pal LR, et al. Protein characterization of a candidate mechanism SNP for Crohn's disease: the macrophage stimulating protein R689C substitution. *PLoS One.* 2011;6:e27269.
33. Willing B, Halfvarson J, Dicksved J, et al. Twin studies reveal specific imbalances in the mucosa-associated microbiota of patients with ileal Crohn's disease. *Inflamm Bowel Dis.* 2009;15:653–660.
34. Travassos LH, Carneiro LA, Ramjeet M, et al. Nod1 and Nod2 direct autophagy by recruiting ATG16L1 to the plasma membrane at the site of bacterial entry. *Nat Immunol.* 2010;11:55–62.
35. Cooney R, Baker J, Brain O, et al. NOD2 stimulation induces autophagy in dendritic cells influencing bacterial handling and antigen presentation. *Nat Med.* 2010;16:90–97.
36. Tremelling M, Berzuini C, Massey D, et al. Contribution of TNFSF15 gene variants to Crohn's disease susceptibility confirmed in UK population. *Inflamm Bowel Dis.* 2008;14:733–737.
37. Thiébaut R, Kotti S, Jung C, et al. TNFSF15 polymorphisms are associated with susceptibility to inflammatory bowel disease in a new European cohort. *Am J Gastroenterol.* 2009;104:384–391.
38. Yang SK, Lim J, Chang HS, et al. Association of TNFSF15 with Crohn's disease in Koreans. *Am J Gastroenterol.* 2008;103:1437–1442.

nature COMMUNICATIONS

ARTICLE

Received 7 Sep 2012 | Accepted 28 Feb 2013 | Published 3 April 2013

DOI: 10.1038/ncomms2668

Microbiota-derived lactate accelerates colon epithelial cell turnover in starvation-refed mice

Toshihiko Okada[1,2], Shinji Fukuda[3,4,†], Koji Hase[4,5,†], Shin Nishiumi[6], Yoshihiro Izumi[6], Masaru Yoshida[6,7], Teruki Hagiwara[1], Rei Kawashima[1,†], Motomi Yamazaki[1], Tomoyuki Oshio[1,†], Takeshi Otsubo[1], Kyoko Inagaki-Ohara[1], Kazuki Kakimoto[1,2], Kazuhide Higuchi[2], Yuki I. Kawamura[1], Hiroshi Ohno[3,4] & Taeko Dohi[1,8]

Oral food intake influences the morphology and function of intestinal epithelial cells and maintains gastrointestinal cell turnover. However, how exactly these processes are regulated, particularly in the large intestine, remains unclear. Here we identify microbiota-derived lactate as a major factor inducing enterocyte hyperproliferation in starvation-refed mice. Using bromodeoxyuridine staining, we show that colonic epithelial cell turnover arrests during a 12- to 36-h period of starvation and increases 12–24 h after refeeding. Enhanced epithelial cell proliferation depends on the increase in live *Lactobacillus murinus*, lactate production and dietary fibre content. In the model of colon tumorigenesis, mice exposed to a carcinogen during refeeding develop more aberrant crypt foci than mice fed *ad libitum*. Furthermore, starvation after carcinogen exposure greatly reduced the incidence of aberrant crypt foci. Our results indicate that the content of food used for refeeding as well as the timing of carcinogen exposure influence the incidence of colon tumorigenesis in mice.

[1] Department of Gastroenterology, Research Center for Hepatitis and Immunology, Research Institute, National Center for Global Health and Medicine, 1-7-1 Kohnodai, Ichikawa, Chiba 272-8516, Japan. [2] Second Department of Internal Medicine, Osaka Medical College, 2-7 Daigakumachi, Takatsuki, Osaka 569-8686, Japan. [3] Laboratory for Epithelial Immunobiology, RIKEN Research Center for Allergy and Immunology, 1-7-22 Suehiro-cho, Tsurumi-ku, Yokohama, Kanagawa 230-0045, Japan. [4] Graduate School of Nanobioscience, Yokohama City University, 1-7-29 Suehiro-cho, Tsurumi-ku, Yokohama, Kanagawa 230-0045, Japan. [5] Bioenvironmental Epigenetics, 1-7-22 Suehiro-cho, Tsurumi-ku, Yokohama, Kanagawa 230-0045, Japan. [6] Division of Gastroenterology, Department of Internal Medicine, Kobe University Graduate School of Medicine, 7-5-1 Kusunoki-cho, Chuo-ku, Kobe, Hyogo 650-0017, Japan. [7] Division of Metabolomics Research, Department of Internal Medicine, Kobe University Graduate School of Medicine, 7-5-1 Kusunoki-cho, Chuo-ku, Kobe, Hyogo 650-0017, Japan. [8] Open Laboratory for Allergy Research, RIKEN Research Center for Allergy and Immunology, 1-7-22 Suehiro-cho, Tsurumi-ku, Yokohama, Kanagawa 230-0045, Japan. † Present addresses: Institute for Advanced Biosciences, Keio University, 246-2 Mizukami, Kakuganji, Tsuruoka, Yamagata 997-0052, Japan (S.F); Division of Mucosal Barriology, The Institute of Medical Science, The University of Tokyo, 4-6-1 Shirokanedai, Minato-ku, Tokyo 108-8639, Japan (K.H); Kitasato University Graduate School of Medical Sciences, 1-15-1 Kitasato, Minami-ku, Sagamihara, Kanagawa 252-0373, Japan (R.K); Department of Dermatology, Jichi Medical University, 3311-1 Yakushiji, Shimotsuke, Tochigi 329-0498, Japan (T.O). Correspondence and requests for materials should be addressed to T.D. (email: dohi@ri.ncgm.go.jp).

The gastrointestinal (GI) tract must adapt to drastic changes in the lumenal environment to maintain homoeostasis, and responses to ingested food are the most fundamental physiological adaptations. Epithelial cells (EC) in the GI tract undergo rapid self-renewal, with a new gut lining produced approximately every 3 days[1]. However, the turnover rate is not always constant. For example, gut EC proliferation rates undergo circadian fluctuation in rodents[2,3] and humans[4,5], which alters the morphology and function of the GI tract. In the normal human rectal biopsies, ^{3}H-thymidine incorporation into cells is higher at night and lower in the afternoon[5]. This circadian rhythm is controlled by clock genes in the central nervous system, as well as local expression of clock genes in intestinal tissue. EC proliferation rates also vary in a longer time span. For example, the GI tract of animals becomes atrophic during hibernation but undergoes rapid recovery on food intake after hibernation[6,7]. To illustrate, snakes usually eat after starvation of several months. On food intake, the snake intestine doubles in wet and dry mass within 1 day, largely as a result of a sixfold increase in microvillus length and a doubling of mucosal EC volume[8]. Thus, oral food intake should greatly change the rate of intestinal cell turnover. In nocturnal rodents, daytime feeding is a strong synchronizer of GI clock genes[9]. In rats, starvation reduces the weight and thickness of the small intestine[10]. In humans, total parenteral nutrition causes atrophy of intestinal mucosa[11,12]. Therefore, oral food intake is necessary for maintenance of cell proliferation and has the highest impact on the morphology and function of the GI tract. However, the mechanisms underlying how food intake regulates EC proliferation are not fully elucidated. In particular, there are few reports about how food intake affects colonic EC proliferation.

Colonic EC turnover is slower than cell turnover in the small intestine. One reason may be the major difference in the luminal environments of the small and large intestines. Nutrients are mostly digested and absorbed in the small intestine, whereas the colon is colonized by microbiota. Thus, instead of orally ingested nutrients taken in by the host, the colon lumen is rich in microbial metabolites and fermentation products produced by the microbiota. As a result, colonic EC rely heavily on fermentation products of intestinal microorganisms, including butyric acid, as a source of carbon and energy[13]. The quality of nutrients for colonic EC is thus associated with the microbiota 'enterotype'[14,15] of the host and may also be associated with the incidence of diseases in the GI tract, including colorectal cancer, as well as diseases affecting other organs[16].

In this study, we found that starvation arrested colon EC turnover, and refeeding induced hyperproliferation in mice. The enhanced EC proliferation was dependent on the microbiota, more specifically lactobacilli and their metabolite lactic acid, which likely supported energy production in EC. We also found that this shift of EC turnover rate by starvation-refeeding dramatically changed the susceptibility to carcinogen exposure.

Results

Transient proliferation of colonic EC in refed mice. We first evaluated the EC turnover of the small and large intestines on starvation and refeeding by quantifying bromodeoxyuridine (BrdU) incorporation into EC. After 36 h of starvation, the number of BrdU + cells in both the small intestine and colon was less than in non-starved controls (Supplementary Fig. S1a), but the difference was only statistically significant in the colon (Fig. 1a,b). Cell turnover in the small intestine recovered to the level of non-starved control mice by 2 h after refeeding. In contrast, in the colon, recovery of cell proliferation was not seen until 6 h after refeeding; thereafter, proliferation exceeded control levels by approximately threefold at 12 h. This excessive cell proliferation continued for 24 h and returned to basal levels by 76 h after refeeding (Fig. 1). In spite of the increased number of proliferating cells, there was no apparent change in the thickness

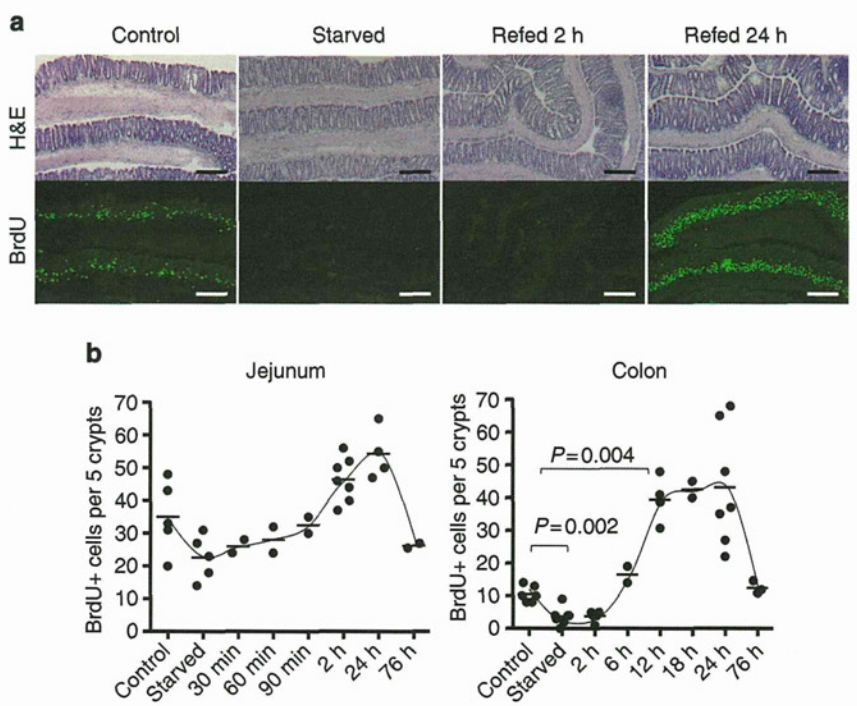

Figure 1 | Starvation-refeeding induced transient colonic EC hyperproliferation. (**a**) Colonic tissues were taken from mice fed *ad libitum* (control), mice starved for 36 h and mice starved for 36 h and refed with normal bait (CE2) for 2 or 24 h. Frozen sections were stained with hematoxylin and eosin (H&E; upper) and anti-BrdU antibody (lower, green). Scale bar, 200 μm. (**b**) Number of BrdU + cells per five crypts was counted at each time point. Each dot indicates an individual mouse. Mann–Whitney test was performed for *P*-value.

of the colonic mucosa. However, the frequency of apoptosis detected with terminal deoxynucleotidyl transferase dUTP nick-end labelling (TUNEL) staining was not increased when compared with control mice fed *ad libitum*, whereas TUNEL$^+$ cells were very rare and found only in luminal surface EC (Supplementary Fig. S1b). This indicated that mucosal thickness did not change significantly because of an appropriately balanced rate of cell turnover, that is, enhanced proliferation with increased shedding rate of EC. This transient hyperproliferation of colonic EC was observed in several mouse strains, irrespective of gender or age (Supplementary Fig. S2a–c). We also found that starvation for only 12 h was sufficient to evoke the same refeeding-induced hyperproliferation response (Supplementary Fig. S2d). Thus, even transient starvation has a substantial impact on colonic EC turnover. Because a 12-h starvation period would be expected to occur on a daily basis, we also examined the daily changes in colonic EC proliferation without a controlled starvation period. As expected, considerable fluctuation in the number of BrdU+ cells was observed (Supplementary Fig. S2e). A high number of proliferating cells, comparable to the increased proliferation observed in refed mice, was seen at approximately noon in our facility. This observation does fit with mice being more active and feeding during the dark cycle and falling asleep (and presumably fasting) during the light cycle.

Because significantly increased EC proliferation was seen in the colon but not in the small intestine, we hypothesized that microbiota may be involved in the underlying mechanisms. Presence of microbiota stimulates innate immune responses through bacterial components, as well as fermentation products. To test the importance of the microbiota for EC proliferation responses to starvation-refeeding, mice were given oral antibiotics. Hyperproliferation in the colon was not observed in mice treated with antibiotics, although recovery of the small intestine was unaffected (Fig. 2a). As fermentation of dietary fibre depends on the action of microbiota, we also eliminated fibre from the mouse diet using a powdered formula of oral rehydration solution (ORS) containing glucose and salt, or an elemental diet containing dextran with amino acids and other nutritional supplements for refeeding after starvation. The small intestinal cell turnover in treated mice was similar to mice fed with normal bait (CE2). However, hyperproliferation in the colon did not take place in the absence of dietary fibre (Fig. 2a). The importance of microbiota in refeeding-induced colonic hyperproliferation was further confirmed in germ-free mice. In these mice, starvation-refeeding induced the transient decrease in BrdU$^+$ cells with subsequent recovery in the small intestine similar to that observed in specific pathogen-free (SPF) mice. However, the refeeding-induced colonic hyperproliferation was not observed in germ-free mice (Fig. 2b), consistent with the results obtained from SPF mice treated with antibiotics. From these results, we conclude that accelerated colonic EC turnover after starvation-refeeding is triggered by a microbiota-dependent mechanism. Lack of hyperproliferation in ORS or elemental diet refed mice suggests that degradation products of dietary fibre by live bacteria are required to support the hyperproliferation response.

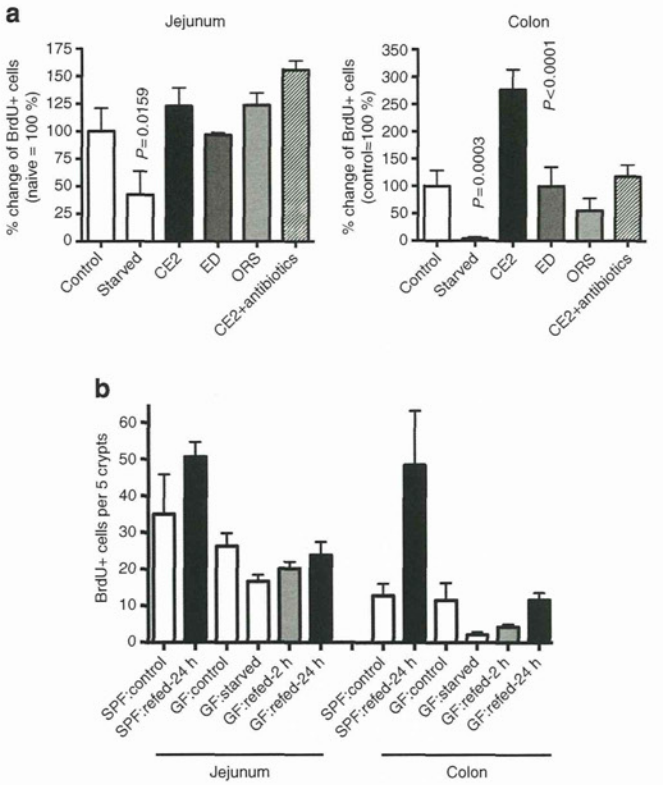

Figure 2 | Requirement for live microbiota and dietary fibre for refed-induced hyperproliferation. (**a**) Mice were starved for 36 h and refed with CE2, ED or ORS. A group of mice refed with CE2 was also given oral antibiotics. The percentage of BrdU+ cells per crypt in the colon 12 h after refeeding was compared (control = 100%). Data are shown as an average + s.d. for 4–6 mice for each group. Statistically significant differences from the control group are indicated with a *P*-value (Mann-Whitney test). (**b**) Germ-free mice were starved for 36 h and refed CE2 for the indicated time. Data are shown as an average + s.d. for three mice for each group.

***Lactobacillus murinus* induced accelerated EC turnover.** The importance of microbiota in refeeding-induced colonic hyperproliferation prompted us to investigate possible alterations in the composition of microbiota during starvation and refeeding. The number of bacteria decreased in both the small and large intestines after starvation. Bacterial numbers recovered to ~50% of baseline at 24 h in the small intestine of mice refed either CE2 or ORS. In contrast, the number of bacteria was approximately twofold greater in the colons of refed animals than in the colons of untreated controls (Fig. 3a). Thus, bacterial outgrowth occurred in the refed-phase concomitant with hyperproliferation in the colon. In fluorescence *in situ* hybridization (FISH) using a universal probe for the bacterial 16S rRNA sequence, overgrown bacteria adhered onto the surfaces of the EC, even in the deep pits of the crypts, which was not observed in control mice (Fig. 3b). However, bacterial translocation across the EC layer was not observed using FISH. The composition of the microbiota analyzed by denaturing gradient gel electrophoresis (DGGE) demonstrated that *Lactobacillus murinus* was a major species in the small intestines of control mice, which disappeared after starvation (Supplementary Fig. S3). The bacterium related to *Streptococcus alactolyticus* was detected in the small intestines of animals starved or refed for 2 h, and *L. murinus* reappeared in either CE2- or ORS-refed mice. In the colon, appearance of *L. murinus* was detected only in CE2-refed mice but not in control, starved or ORS-refed mice (Fig. 3c). Further, starvation-refeeding experiments using gnotobiotic mice monoassociated with *L. murinus* showed that presence of *L. murinus* alone was able to reconstitute colonic EC hyperproliferation in refed mice (Fig. 3d,e). Thus, colonic EC hyperproliferation on refeeding seems tightly associated with the outgrowth of *L. murinus*.

Lactate and *L. murinus*-induced EC hyperproliferation. To identify the inducer of colonic EC hyperproliferation, we

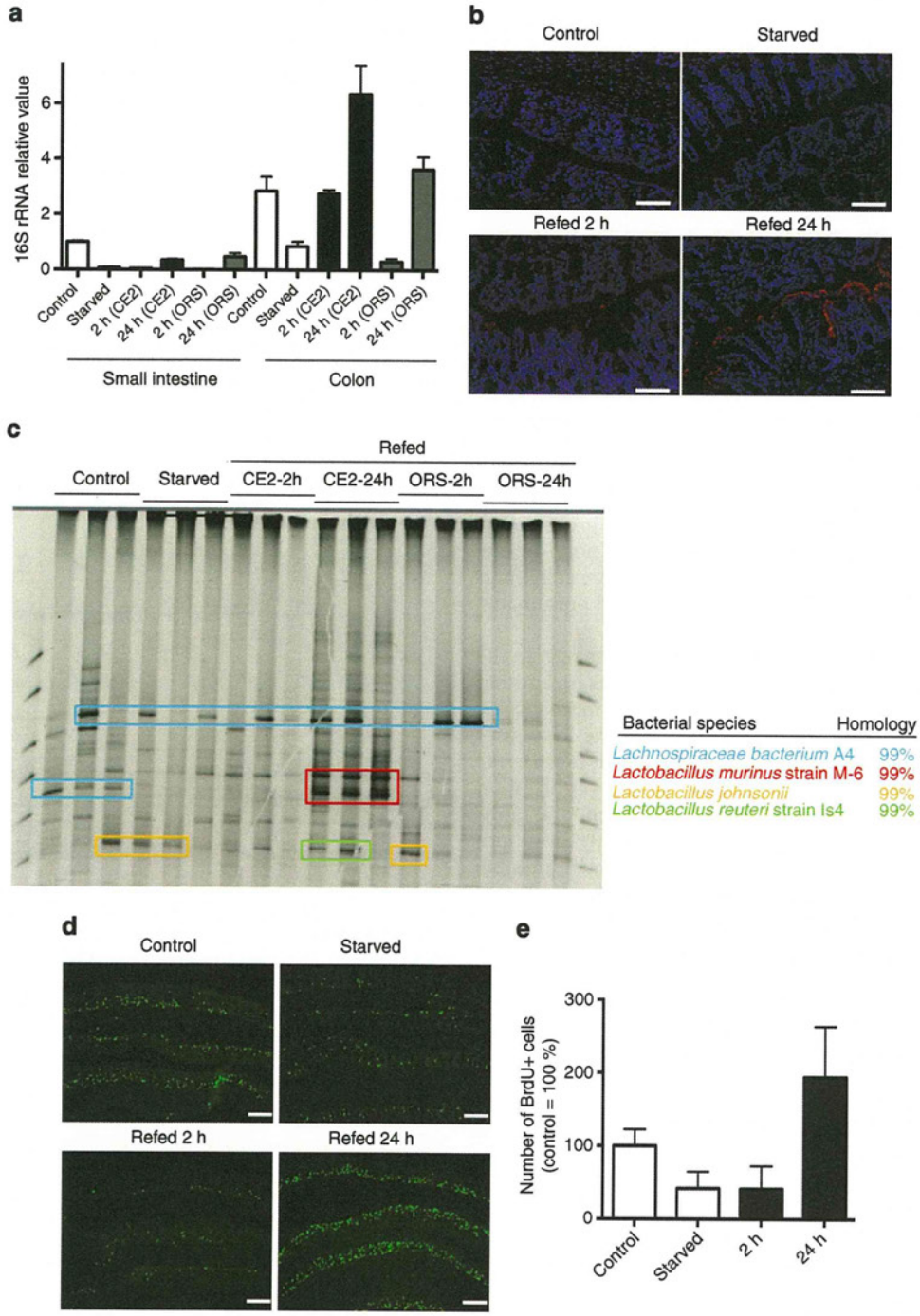

Figure 3 | Colonic EC hyperproliferation is induced by *Lactobacillus murinus*. (**a**) Number of bacteria determined by the 16S rRNA value. Mice were starved for 36 h and refed with the indicated formula in parentheses for the indicated time duration. Data are shown as an average + s.d. for three mice for each group. (**b**) FISH analysis of the starvation-refed colon with the 16S RNA probe. Scale bar, 100 μm. (**c**) DGGE analysis of colonic luminal contents in control mice and mice starved for 36 h and refed with CE2 or ORS for 2 or 24 h. Colonic luminal contents were collected and the microbial species determined, as described in the Methods. Each lane represents samples from individual mice. (**d**) Gnotobiotic mice were generated by inoculation of *Lactobacillus murinus* into germ-free mice. Frozen sections were stained by anti-BrdU antibody (green). Scale bar, 200 μm. (**e**) Number of BrdU + cells is shown as relative to control gnotobiotic mice. Data are shown as an average + s.d. for three mice for each group.

attempted to reconstitute hyperproliferation in ORS-refed mice. As shown in Fig. 4a, we first confirmed that intrarectal injection of fresh caecal contents from starvation-CE2-refed mice into ORS-refed mice fully induced hyperproliferation, demonstrating that intestinal luminal contents are critical for the hyperproliferation response. Rectal administration of ultraviolet-killed total flora or *L. murinus* (1×10^{10} colony-forming units, 0.1 ml per mouse) only partially reconstituted CE2-refed hyperproliferation, suggesting that live bacterial metabolites may be required for the full response. To identify the hyperproliferation-inducing factor(s), metabolome analysis of the colonic luminal contents was performed using a gas chromatography–mass spectrometry (GC–

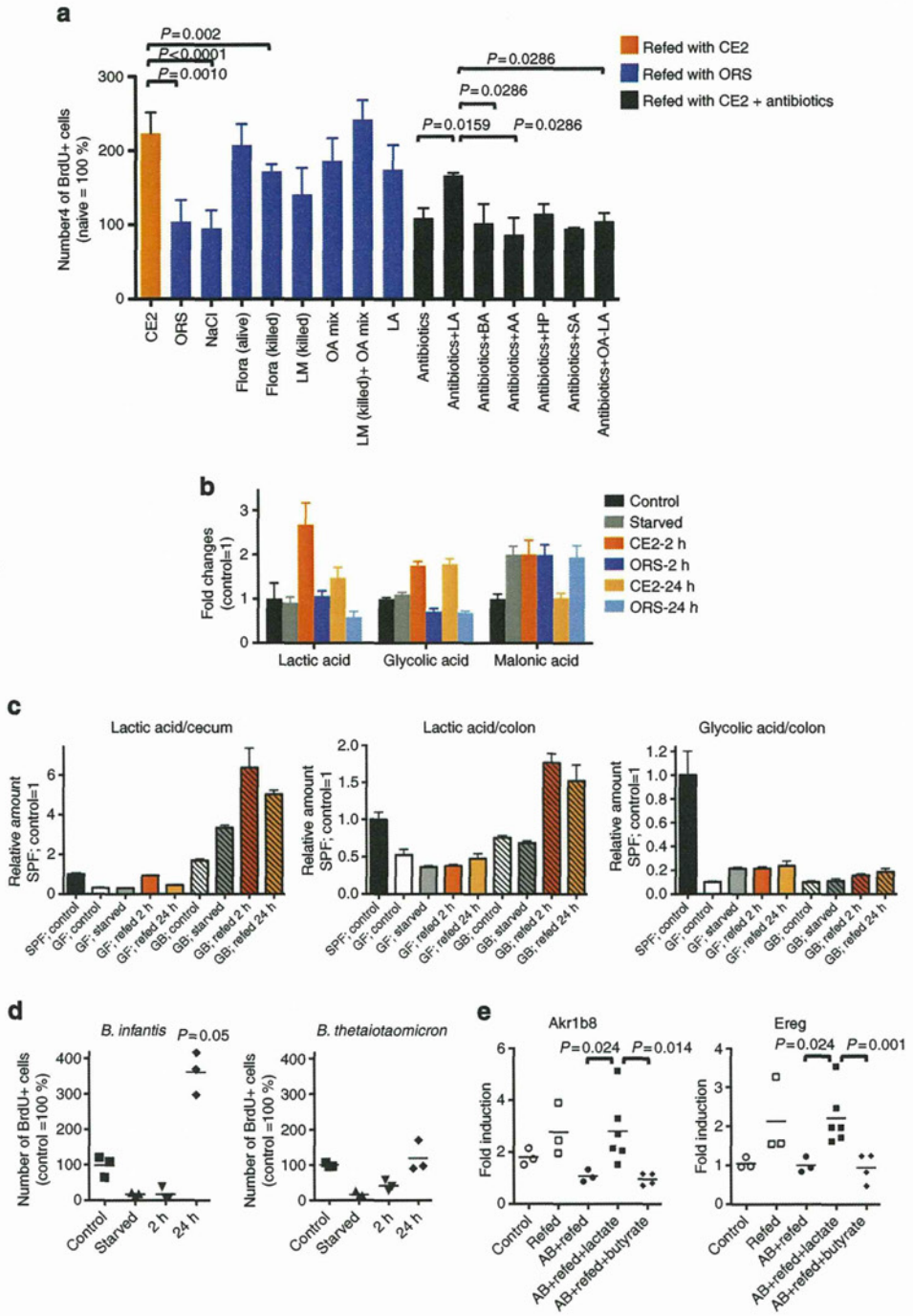

Figure 4 | Lactate is required for hyperproliferation. (**a**) Mice were starved for 36 h and refed CE2 (orange) or ORS (blue) or CE2 with oral antibiotics (black) for 12 h. In ORS-refed mice, the number of BrdU+ cells in the colon without rectal injection (ORS), with rectal injection of control 500 mM NaCl (NaCl), fresh caecal contents from CE2-refed mice (flora-alive), killed flora (flora-killed), killed *L. murinus* (LM-killed), organic acid mixture (OA mix), LM-killed plus organic acid mixture (LM-killed + OA mix), 500 mM lactate (LA) or a combination of these are shown. In mice refed with CE2 and treated with oral antibiotics, 500 mM NaCl (antibiotics), lactate (LA), butyrate (BA), acetate (AA), 3-hydroxypropionate (HP), succinate (SA) or OA mixture minus lactate (OA − LA) was administered intrarectally together with antibiotics three times during refeeding. Data are shown as the average + s.d. of 3–7 mice relative to control (fed *ad libitum*) mice. (**b**) Typical patterns of metabolome analysis as relative changes from the control condition. Data are shown as the average + s.d. of three mice as the relative signal intensity to control SPF mice. (**c**) Relative amount of lactic acid in the caecum and colon, and glycolic acid in the colon from starvation-refed, germ-free (GF) and gnotobiotic mice monoassociated with *L. murinus* (GB, hatched). Data are shown as the mean + s.d. of three mice as the relative signal intensity to control SPF mice. (**d**) Number of BrdU+ cells in the colon of gnotobiotic mice monoassociated with lactate-producing *Bifidobacterim infantis* or non-lactate-producing *Bacteroides thetaiotaomicron* shown as % of control (fed *ad libitum*). Short bar indicates the mean value. (**e**) Gene expression in the colon. Mice were starved for 36 h and refed CE2. Some mice were treated with oral antibiotics (AB), and 500 mM lactate or butyrate was administered intrarectally together with antibiotics three times during refeeding. After 12 h of refeeding, distal 1/3 of the colon was subjected to total RNA extraction and quantitative RT-PCR for Akr1b8 and Ereg. Data were shown as relative expression (AB + refed = 1). Each dot represents individual mice, and short bar indicates the mean value. In panels **a**, **d** and **e**, *P*-values were calculated using Mann–Whitney test.

MS) system (Supplementary Fig. S4). Some amino acids were markedly decreased in starved mice and recovered to control levels on refeeding with either CE2 or ORS, except aspartic acid, asparagines and glutamine, which did not return to control levels in ORS-refed mice. We found that organic acids were classified into at least two groups according to the pattern of alteration during starvation-refeeding. One group increased in CE2-refed mice but not in ORS-refed mice, which included lactic acids, glycolic acid, 3-hydroxypropanoic acid, maleic acid, glutaric acid, 2-deoxytetronic acid, 3-hydroxyphenylacetic acid and 4-hydroxybenzoic acid. The second group increased in starved mice and decreased after CE2-refeeding but not after ORS-refeeding, and included caproic acid, 2-hydroxybutyric acid, 2-hydroxyisovaleric acid, 4-hydroxyphenylacetic acid and malonic acid. Representative organic acids of these two groups are shown in Fig. 4b. Most fatty acids analyzed and urea showed similar kinetic patterns to the second group of organic acids (Supplementary Fig. S4). As we found that live *Lactobacillus* and its metabolite(s) were required for colonic EC hyperproliferation, we hypothesized that organic acids that increased on refeeding (that is, the first group) were most likely associated with EC hyperproliferation. On the basis of the total ion peak values of the GC–MS analysis (Supplementary Fig. S5a) and a separate analysis of luminal contents using NMR from control mice (Supplementary Fig. S5b), the composition of organic acid was estimated. According to these results, a mixture containing acetic acid, propionic acid, butyric acid, lactic acid, 3-hydroxypropionic acid, glycolic acid, succinic acid and glyceric acid was tested for its ability to support EC hyperproliferation on refeeding. This mixture induced hyperproliferation (that is, increased the number of $BrdU^+$ cells) more efficiently than ultraviolet-killed *L. murinus*, and co-administration of this mixture with killed bacteria induced the full hyperproliferative response (Fig. 4a). As *L. murinus* produces mainly lactate, we treated ORS-refed animals with 500 mM lactate alone rectally and examined colonic EC proliferation. Lactate alone resulted in EC hyperproliferation comparable to that of the organic acid mixture, indicating that this component was largely responsible for the observed response. To further confirm the action of lactic acid, mice refed with CE2 were treated orally and rectally with antibiotics and either lactate, butyrate, acetate, 3-hydroxypropanoate and succinate. As shown in Fig. 4a, only lactate induced EC hyperproliferation on refeeding, and deletion of lactate from the organic acid mixture resulted in the loss of hyperproliferation. This indicated that lactate was the most important organic acid for stimulation of colonic EC turnover in response to starvation-refeeding. Indeed, in germ-free mice, there were no significant changes in the amount of lactic acid during starvation-refeeding, while increased lactic acid was evident in the cecums and colons of *L. murinus*-monoassociated mice on refeeding (Fig. 4c). Glycolic acid, which also increased in the refed colons of SPF mice (Fig. 4b), did not change significantly on starvation-refeeding in germ-free mice and there were no differences in the levels of glycolic acid between germ-free and *L. murinus*-monoassociated mice. In summary, outgrowth of *L. murinus* and, therefore, production of lactic acid, induced the hyperproliferation of colonic EC. To further confirm this finding, we prepared gnotobiotic mice monoassociated with lactate-producing *Bifidobacterim longum* subsp. *infantis* (*B. infantis*) and non-lactate-producing *Bacteroides thetaiotaomicron* (*B. thetaiotaomicron*)[17,18]. As shown in Fig. 4d, starvation-refed *B. infantis*-monoassociated mice demonstrated hyperproliferation at refeeding. On the other hand, *B. thetaiotaomicron* did not induce hyperproliferation. These results clearly demonstrate that a bacterial metabolite (lactate) rather than bacterial components has a major role to induce accelerated cell turnover.

Upregulation of energy production pathway in refed colon EC. To characterize the signature of hyperproliferative EC induced by refeeding, we compared the gene expression profiles of purified EC derived from refed mice and refed mice treated with antibiotics. Pathway analysis showed that genes increased 1.5-fold in refed EC than in refed EC treated with antibiotics indicated the enrichment of the genes related to energy production, lipid metabolism, small-molecule biochemistry as the top networks, and glycerolipid metabolism as the top canonical pathway as shown in Tables 1 and 2 and in Supplementary Figs S6 and S7. This finding indicates that refed EC actively produce energy using stored fat. The glycerolipid metabolism pathway shown in Supplementary Fig. S7 clearly indicated increased fatty acid release from glycerolipids. The fatty acids that underwent beta-oxidation into acetyl CoA can eventually enter the tricarboxylic acid cycle to produce ATP, suggesting that the presence of luminal lactate facilitates ATP production through enhanced use of lipids.

To confirm that this gene expression profile is related to lactate in the lumen, we attempted to validate the result with quantitative PCR with reverse transcription (RT–PCR) using fresh colon exposed to lactate. *Akr1b8*, encoding aldo-keto reductase family 1, member B8, listed as enzyme commission number 1.1.1.21 in Supplementary Fig. S7, was one of top 10 genes enriched in refed colon (Supplementary Fig. S8). *Ereg* encodes epiregulin, a member of epidermal growth factor family and 1.7-fold higher in refed colon than that treated with antibiotics (Supplementary Fig. S8). As shown in Fig. 4e, both gene levels tended to be higher in refed mice than those of mice fed *ad libitum* (control). This upregulation was not seen in refed mice treated with antibiotics; However, additional rectal injection of lactate significantly upregulated both genes. Butyrate failed to induce expression of these genes in

Table 1 | Top five gene networks of 1.5-fold upregulated genes in colonic EC from refed mice compared with refed mice treated with antibiotics.

Associated network functions	Score
Energy production, lipid metabolism, small-molecule biochemistry	50
Cell death, reproductive system development and function, haematological disease	39
Post-translational modification, carbohydrate metabolism, lipid metabolism	29
Lipid metabolism, small-molecule biochemistry, vitamin and mineral metabolism	27
Lipid metabolism, small-molecule biochemistry, molecular transport	26

Table 2 | Top five canonical pathways of 1.5-fold upregulated genes in colonic EC from refed mice compared with refed mice treated with antibiotics.

Top canonical pathways	*P*-value*
Glycerolipid metabolism	1.04E-06
Metabolism of xenobiotics by cytochrome P450	2.23E-05
Linoleic acid metabolism	2.46E-05
LPS/IL-1-mediated inhibition of RXR function	3.33E-05
Arachidonic acid metabolism	3.24E-04

*The generated canonical pathways were ranked by *P*-values, which were calculated using a Fisher's exact test by comparing the number of the selected genes relative to the total number of occurrences of these genes in all functional/pathway annotations stored in the Ingenuity Pathways Knowledge Base.

antibiotic-treated mice. These results further support the notion that lactate changes the gene expression of EC and drives metabolic shift to enhance cell proliferation in refed mice.

Starvation-refeeding alters susceptibility to carcinogen. Our observation that colonic EC turnover is accelerated after starvation-refeeding in the presence of microbiota prompted us to test whether this proliferative response to refeeding sensitizes colonic EC to tumorigenesis. To this end, we employed a mouse model of tumorigenesis using the chemical carcinogen azoxymethane (AOM), which induces aberrant crypt foci (ACF) of the colon. The experimental protocol is illustrated in Supplementary Fig. S9. In mice given AOM 8 h after the initiation of refeeding, at the beginning of hyperproliferation of the colon, the number of ACF was significantly higher than in mice fed *ad libitum* (Fig. 5a). In contrast, when mice were challenged with AOM followed by starvation and refeeding, it resulted in a striking decrease in the number of ACF (Fig. 5a). In addition to ACF, the colonic mucosa of refed-plus AOM mice appeared rough and scraggly (Fig. 5b), matching the histological image, in which the deformed and atypical shapes of the crypts were scattered (Fig. 5c); however, crypts of mice with AOM followed by starvation had a smooth appearance (Fig. 5b) lined with goblet cells (Fig. 5c). As we thought that hyperproliferation was responsible for the increased number of ACF in refed-plus AOM mice, oral antibiotics were administered to AOM-treated mice during refeeding to block the production of lactic acid by *L. murinus* and thereby prevent EC hyperproliferation. This treatment reduced the number of ACF to that of control mice and decreased the irregularities observed in the colonic mucosa (Fig. 5a,c). These observations suggest that hyperproliferation in response to refeeding increases the number of AOM-susceptible cells, resulting in a greater number of ACF. In contrast, accelerated cell turnover after temporal starvation appears to eliminate damaged cells efficiently. Although AOM metabolism may drastically change during starvation and refeeding, expression levels of CYP2E1, a major enzyme associated with the activation of AOM, did not correlate with the number of ACF (Supplementary Fig. S9b). We think the metabolic rate of AOM is not a major factor that distinguishes sensitivity to DNA damage between starved and refed mice (Supplementary Discussion).

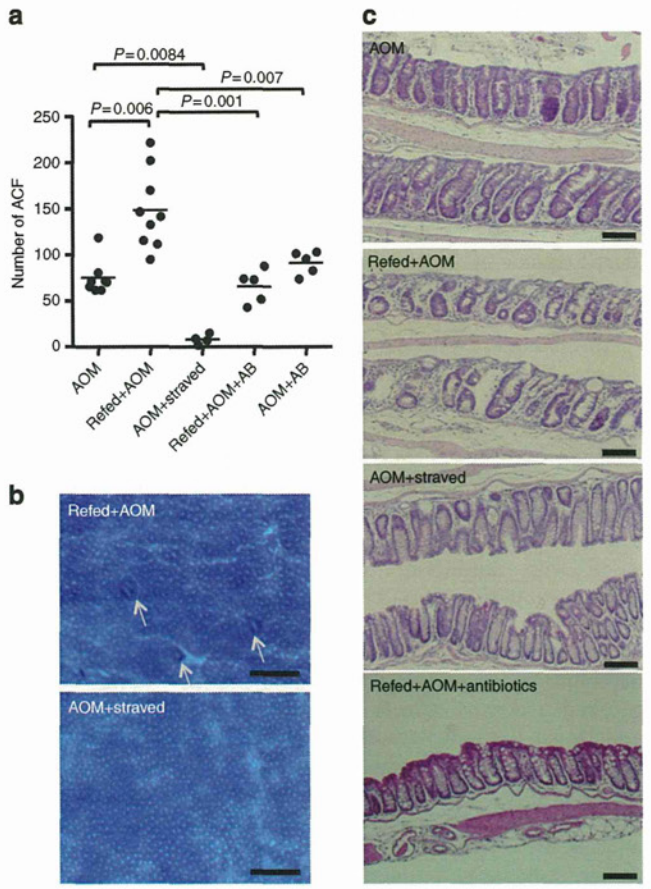

Figure 5 | Effects of starvation-refeeding on exposure to carcinogen. (**a**) The number of ACF in the colon. AOM, mice fed *ad libitum* and treated with AOM; Refed + AOM, treatment with AOM at refeeding; AOM + starved, mice fed *ad libitum* and treated with AOM, then starvation was begun on the following day; Refed + AOM + AB, refed + AOM mice were treated with oral antibiotics; AOM + AB, mice were fed *ad libitum* and treated with AOM and oral antibiotics. These treatments were repeated five times a week. A week after the last injection of AOM, ACF in the colon were quantified. Each dot indicates an individual mouse. *P*-values were calculated using Mann–Whitney test. For a detailed protocol, see Supplementary Fig. S9. (**b**) Methylene blue staining of the colon from Refed + AOM or AOM + starved mouse groups. Arrows indicate ACF. Images were captured with a stereomicroscope. Scale bar, 0.5 mm. (**c**) Formalin-fixed paraffin-embedded sections were stained with H&E. Scale bar, 100 μm. All images were taken from the same region of the colon (distal one-third).

Discussion

In this study, we found that transient starvation enhanced EC turnover on refeeding, and this response was dependent on the presence of commensal lactobacilli and its metabolite, lactate. We also found that carcinogen sensitivity was significantly increased during refeeding and was reduced by starvation after exposure to the carcinogen.

There are a limited number of studies on colonic EC turnover during starvation. Using the metaphase-arrest technique, it has been reported that there is reduced 'crypt cell production' during starvation and an 'overshooting' recovery after refeeding[2]; in rats, colonic EC responses are dependent on the presence of fermentable fibre[19]. Taken together with our results, these data indicate that our observations are not particular to our animal facility or animals colonized with certain microbiota. In this study, we identified lactic acid-producing *L. murinus* as the causal factor for the refeeding EC hyperproliferation response. As discussed below, because lactate was sufficient to accelerate EC turnover, many lactic acid-producing bacteria have the potential to induce a similar effect.

In our study, *L. murinus* was detected in control (fed *ad libitum*) conditions in the small intestine but was not a dominant strain in the colon at steady state. In some individual control mice, *L. murinus* was a major strain in the small intestine. In contrast, outgrowth of *L. murinus* was universally observed in the colons of refed mice. When the results of Fig. 3a–c are considered, *L. murinus* appeared to be the major constituent of refed colonic microbiota, apparently heavily attached to the mucosal surface. While *L. murinus* did reside in the small intestine before starvation, its outgrowth in the colon on starvation-refeeding was likely due to the luminal environment becoming particularly suitable for its growth. Colonization of *L. murinus* may be affected by changes in available nutrients, oxygen concentration, or host and microbial factors for adhesion, such as production and carbohydrate structure of host mucins, secretion of host antibacterial peptides and upregulation of microbial adhesins, including mucus-binding protein[20]. Indeed, luminal nutrients changed dramatically during starvation, and loss of villi in the small intestine reduced the available surface area for

bacterial adhesion. All these changes may have favored the growth of *L. murinus* in the refed colon. Refeeding with ORS provides glucose as the energy source, which may not reach the colon lumen, sustains morphological recovery of small intestine EC. However, ORS-refeeding failed to support *L. murinus* colonization or hyperproliferation of colonic EC. In the experiment using gnotobiotic mice, we showed that monoassociation with *L. murinus* was sufficient to induce colonic EC hyperproliferation in refed mice. Therefore, we conclude that outgrowth of *L. murinus* induced colonic EC hyperproliferation on refeeding.

In subsequent experiments, we identified lactate as the most important *L. murinus* metabolite for the induction of colon hyperproliferation. This conclusion is based on several pieces of evidence. First, metabolome analyses indicated that lactic acid levels increased substantially in the colons of CE2-refed animals but not in ORS-refed colons. Second, gnotobiotic mice monoassociated with *L. murinus* had contained elevated lactic acid levels in the colon, and gnotobiotic mice monoassociated with a lactate-producing stain but not a non-lactate-producing strain showed hyperproliferation after starvation. Third, in animals treated with antibiotics to eliminate normal flora, rectal administration of lactic acid but not butyrate or acetate supported colonic EC proliferation. This result surprised us, because butyrate and acetate are also major fermentation products of microbiota, and there is a wide range of evidence supporting their beneficial protective effects on colonic EC[21–25]. On the other hand, lactate has long been considered a dead-end waste product; however, some recent studies have shown that lactate has diverse metabolic and regulatory properties, such as being an energy source, a modulator of energy production, and a signalling molecule for cell repair and angiogenesis (reviewed in ref. 26). Further, survival and function of some types of cells such as neurons and germ cells that demand high energy depend on the extracellular lactate provided by adjacent nursing cells, astrocytes and Sertoli cells[27]. Although we did not obtain direct evidence that lactate itself is used as an energy source, we speculate that the modified redox status of EC by starvation-refeeding might enable EC to respond to luminal lactate to promote energy production.

On the basis of these observations, we posed the question, 'What is the significance of colonic hyperproliferation on refeeding to health and disease?' Treatment of refed animals with AOM clearly demonstrated that exposure to a carcinogen during the colonic hyperproliferation response to refeeding significantly increased the risk of tumorigenesis. In contrast, colonic hyperproliferation induced after exposure to a carcinogen appears to eliminate damaged cells efficiently. In general, starvation or calorie restriction has been reported to extend the lifespan of most species, including rodents and primates. The molecular basis for this observation has been proposed to be sirtuins and the nutritional signalling target of rapamycin pathway[28,29]. Studies also have shown that calorie restriction decreases the risk of colon cancer[30]; however, our study suggests that the timing of carcinogen exposure is a critical factor. After transient starvation, there is a window of time when colonic EC become susceptible to DNA damage, and this greatly depends on the bacterial flora and luminal metabolite composition. Thus, our results provide new insight into the relationship between carcinogenesis, food intake and lifestyle.

Methods

Mice. Six-week-old male BALB/c mice were used for all experiments, unless otherwise indicated. All mice were obtained from CLEA Japan Inc. (Tokyo, Japan), maintained under SPF conditions at the National Center for Global Health and Medicine facility (Tokyo, Japan), and fed normal bait (CE2, Clea Japan). Germ-free mice (BALB/c background) were purchased from Sankyo Labo Service Corporation, Inc. and kept in an animal facility in RIKEN. All experiments were performed according to the Institutional Guidelines for the Care and Use of Laboratory Animals in Research and the approval of the local ethics committee at the National Center for Global Health and Medicine and RIKEN.

Starvation and refeeding. During starvation, mice were kept in plastic cages with bedding chips and drinking water without bait. Irrespective of the length of the starvation period, the refeeding period was set to begin at 8:00 in all experiments. Elementary diet (Elental) was obtained from Ajinomoto Co. Inc.. Powdered formula of ORS contained 675 g glucose, 130 g NaCl, 145 g trisodium citrate dihydrate and 75 g KCl mixed in a sterilized mortar. To eliminate endogenous flora, a 0.2-ml solution of 500 mg l^{-1} metronidazol and 1 g l^{-1} vancomycin was administered daily by oral–gastric gavage. After starvation, 12- and 24-h refeeding with elemental diet or ORS were able to recover body weights comparable to CE2.

In enema experiments, ultraviolet irradiation-killed *L. murinus* was prepared, and pelleted cells were re-suspended in PBS (1×10^{10} colony-forming units; 0.1 ml per mouse). For intrarectal administration of the reagents, 0.1 ml of the indicated solution was injected into the rectum three times within the first 12 h of refeeding (0, 4 and 8 h after refeeding), and animals were lightly anesthetized using inhaled sevoflurane. The organic acid mixture contained 600 mM acetic acid, 200 mM propionic acid, 200 mM butyric acid, 200 mM lactic acid, 200 mM 3-hydroxypropionic acid, 100 mM glycolic acid, 40 mM succinic acid and 200 mM glyceric acid (final concentrations). In some experiments, antibiotics (50 mg l^{-1} metronidazol and 0.1 g l^{-1} vancomycin, final concentration) were added to the solutions for rectal injection.

Microbiological analysis

16S rRNA. Bacterial genomic DNA was isolated as described previously with some modifications[31]. In brief, faecal samples were freeze-dried, homogenized, disrupted using 0.1-mm Zirconia/Silica Beads, and extracted with 10% sodium dodecyl sulphate/Tris-HCl plus ethylenediamine tetraacetic acid (EDTA) buffer solutions. Bacterial genomic DNA was purified from the faecal extracts using a phenol/chloroform/isoamyl alcohol method. Bacterial genomic DNA samples were amplified using SYBR premix Ex Taq (TAKARA BIO, Otsu, Japan) and universal primers for the genes encoding bacterial 16S rRNA[22,32]. The results were calculated as the amount relative to copy number detected in the small intestinal contents of control mice.

DGGE analysis. Bacterial genomic DNA samples were amplified by PCR with universal bacterial primers 954f and 1396r specific for the V6 to V8 regions of the 16S rRNA gene[33]. The reaction mixtures and PCR conditions were described previously[32]. After confirmation of the PCR product by agarose gel electrophoresis, DGGE was performed with the DCode universal mutation detection system (Bio-Rad Lab., Irvine, CA). Polyacrylamide gel conditions for the denaturing gradient, migration, and differentiation were described previously[33]. Electrophoresis was conducted with a constant voltage of 82 V at 60 °C for 15 h. Gels were stained with SYBR Green I (Lonza, Rockland, ME) and acquired by GelDoc XR (Bio-Rad Lab)[31].

Fluorescence in situ hybridization. Bacterial 16s rRNA FISH was performed as described previously[34]. In brief, colonic tissue sections were fixed in 4% paraformaldehyde, washed in PBS, incubated in 50 µl of 30% formamide hybridization buffer containing 25 ng of 5′-Cy3-labelled universal oligonucleotide probes for eubacteria (EUB338, 5′-GCTGCCTCCCGTAGGAGT-3′) or the non-bacterial control (NONEUB, 5′-ACTCCTACGGGAGGCAGC-3′) for 90 min at 46 °C, and washed with the same stringency for 20 min at 48 °C. Stained sections were imaged on a DM-IRE2 confocal laser-scanning microscope (Leica Microsystem).

Metabolome-GC/MS analysis and data processing. Intestinal contents were collected and lyophilized. To extract low-molecular-weight metabolites, 10 mg of lyophilized intestinal contents were transferred to a clean tube and homogenized in 1,000 µl solvent mixture ($MeOH:H_2O:CHCl_3 = 2.5:1:1$). Then, 10 µl of 0.5 mg ml^{-1} 2-isopropylmalic acid (Sigma-Aldrich, Tokyo, Japan) dissolved in distilled water was added to each tube, and the mixture was mixed well. The mixture was shaken at 1,200 r.p.m. for 30 min at 37 °C before being centrifuged at 16,000*g* for 3 min at 4 °C. Nine-hundred microliters of the resultant supernatant were collected into a clean tube. Four-hundred fifty microliters of $CHCl_3$ were added to the collected supernatant and centrifuged at 16,000*g* for 3 min at 4 °C, and 500 µl of supernatant were collected in a clean tube. Two-hundred microliters of distilled water were added to the collected supernatant and centrifuged at 16,000*g* for 3 min at 4 °C; 500 µl of supernatant were collected in a clean tube. The collected supernatant was lyophilized using a freeze-dryer before oximation and the following derivatization. For oximation, 80 µl of 20 mg ml^{-1} methoxyamine hydrochloride (Sigma-Aldrich), dissolved in pyridine, was mixed with a lyophilized sample before being shaken at 1,200 r.p.m. for 90 min at 30 °C. Next, 40 µl *N*-methyl-*N*-trimethylsilyl-trifluoroacetamide (GL Science, Tokyo, Japan) were added for derivatization, and the mixture was incubated at 1,200 r.p.m. for 30 min

at 37 °C. The mixture was centrifuged at 16,000*g* for 5 min at 4 °C, and the resultant supernatant was subjected to GC–MS analysis.

According to our previous reports[35,36], GC–MS analysis was performed using GCMS-QP2010 Plus (Shimadzu Co., Kyoto, Japan) with a DB-5 column (30 m × 0.25 mm inner diameter; film thickness is 1.00 μm, J&W Scientific, Folsom, CA) and GCMS-QP2010 Ultra (Shimadzu Co., Kyoto, Japan) with a CP-SIL 8 CB low-bleed/MS column (30 m × 0.25 mm inner diameter, film thickness is 0.25 μm, Agilent Co., Palo Alto, CA). Processing of data obtained from GCMS-QP2010 Plus and GCMS-QP2010 Ultra was carried out as described previously[35,36]. For semi-quantification, the peak heights of each ion were calculated and normalized using the peak height of 2-isopropylmalic acid as an internal standard.

Metabolome-NMR analysis. NMR-based metabolomics was performed as described previously with minor modifications[37]. In brief, faecal metabolites from mice were extracted by gentle shaking with 100 mM potassium phosphate buffer containing 90% deuterium oxide and 1 mM sodium 2,2-dimethyl-2- silapentane-5-sulfonate as the chemical shift references ($\delta = 0.0$ p.p.m.), and analyzed by ^{1}H-NMR and ^{1}H, ^{13}C-NMR. Metabolite annotations were performed using our standard database[38].

Induction of ACF. As shown in Supplementary Fig. S9, mice were divided into five groups. Group 1 (AOM) was fed *ad libitum* and intraperitoneally injected with AOM (Sigma-Aldrich, 10 mg kg^{-1}). Group 2 (refed + AOM) was starved for 24 h, refed with CE2 and injected with AOM 8 h after refeeding. Group 3 (AOM + starved) was injected with AOM at 16:00; fasting for 24 h was begun at 8:00 on the following day. Group 4 (refed + AOM + AB) was treated similar to Group 2 but oral antibiotics were administered, as described above, beginning with a 5-day starvation period. Group 5 (AOM + AB) was fed *ad libitum*, injected with AOM and given oral antibiotics for 5 days. These protocols were repeated weekly, five times. All mice groups were given AOM injections at 16:00. On day 37, colon tissues were obtained, washed and extended by flushing with PBS. Colons were opened longitudinally, fixed with formalin and stained with 3% methylene blue. ACF were enumerated under a stereomicroscope[39].

Gene expression profiling of colon ECs. For global gene expression profiling in EC, colon tissues were stirred in 6.5 mM dithiothreitol in Hank's Balanced Salt Solution for 15 min at room temperature and in 10 mM EDTA in Hank's Balanced Salt Solution for 10 min. Treatment with EDTA was repeated 4–6 times until EC were released from the stroma. Single-cell suspensions of EC were stained with 7-amino-actinomycin D, fluorescein isothiocyanate-anti-CD45 and phycoerythrin-anti-EpCAM antibodies (BD). Viable EpCAM^{+}CD45^{-} cells were sorted as purified EC (Moflo, Beckman Coulter, Tokyo, Japan). Total RNA was extracted according to standard protocols (Affymetrix). Targets were prepared and hybridized to the GeneChip Mouse Gene 1.0 ST Array (Affymetrix) according to standard protocols. GeneChip data sets were analyzed using GeneSpring GX 11 (Agilent). Array data were normalized using robust multi-array analysis algorithms.

Statistical analysis. All data are presented as the mean ± s.d., unless indicated in the legend. For comparison of two groups, a non-parametric method (Mann–Whitney test) and Student's *t*-test were used in comparisons as indicated in the legends. Results were determined as significant when *P*-values were less than 0.05. Statistical analyses were performed using GraphPad Prism 4 software (GraphPad Software, Inc).

Methods for histological analyses, quantitative RT–PCR, and pathway analysis of gene expression profiling are described in the Supplementary Information.

References

1. Heath, J. P. Epithelial cell migration in the intestine. *Cell Biol. Int.* **20,** 139–146 (1996).
2. Goodlad, R. A. & Wright, N. A. The effects of starvation and refeeding on intestinal cell proliferation in the mouse. *Virchows Arch. B Cell Pathol. Incl. Mol. Pathol.* **45,** 63–73 (1984).
3. Scheving, L. E., Tsai, T. H. & Scheving, L. A. Chronobiology of the intestinal tract of the mouse. *Am. J. Anat.* **168,** 433–465 (1983).
4. Buchi, K. N., Moore, J. G., Hrushesky, W. J., Sothern, R. B. & Rubin, N. H. Circadian rhythm of cellular proliferation in the human rectal mucosa. *Gastroenterology* **101,** 410–415 (1991).
5. Marra, G. *et al.* Circadian variations of epithelial cell proliferation in human rectal crypts. *Gastroenterology* **106,** 982–987 (1994).
6. Carey, H. V. Seasonal changes in mucosal structure and function in ground squirrel intestine. *Am. J. Physiol.* **259,** R385–R392 (1990).
7. Carey, H. V., Andrews, M. T. & Martin, S. L. Mammalian hibernation: cellular and molecular responses to depressed metabolism and low temperature. *Physiol. Rev.* **83,** 1153–1181 (2003).
8. Secor, S. M. & Diamond, J. A vertebrate model of extreme physiological regulation. *Nature* **395,** 659–662 (1998).
9. Hoogerwerf, W. A. *et al.* Clock gene expression in the murine gastrointestinal tract: endogenous rhythmicity and effects of a feeding regimen. *Gastroenterology* **133,** 1250–1260 (2007).
10. Steiner, M., Bourges, H. R., Freedman, L. S. & Gray, S. J. Effect of starvation on the tissue composition of the small intestine in the rat. *Am. J. Physiol.* **215,** 75–77 (1968).
11. Kudsk, K. A. Effect of route and type of nutrition on intestine-derived inflammatory responses. *Am. J. Surg.* **185,** 16–21 (2003).
12. Kudsk, K. A. *et al.* Enteral versus parenteral feeding. Effects on septic morbidity after blunt and penetrating abdominal trauma. *Ann. Surg.* **215,** 503–513 (1992).
13. Roberfroid, M. B., Bornet, F., Bouley, C. & Cummings, J. H. Colonic microflora: nutrition and health. Summary and conclusions of an International Life Sciences Institute (ILSI) [Europe] workshop held in Barcelona, Spain. *Nutr. Rev.* **53,** 127–130 (1995).
14. Arumugam, M. *et al.* Enterotypes of the human gut microbiome. *Nature* **473,** 174–180 (2011).
15. Wu, G. D. *et al.* Linking long-term dietary patterns with gut microbial enterotypes. *Science* **334,** 105–108 (2011).
16. Maslowski, K. M. & Mackay, C. R. Diet, gut microbiota and immune responses. *Nat. Immunol.* **12,** 5–9 (2011).
17. Macfarlane, S. & Macfarlane, G. T. Regulation of short-chain fatty acid production. *Proc. Nutr. Soc.* **62,** 67–72 (2003).
18. Sonnenburg, J. L., Chen, C. T. & Gordon, J. I. Genomic and metabolic studies of the impact of probiotics on a model gut symbiont and host. *PLoS Biol.* **4,** e413 (2006).
19. Goodlad, R. A. *et al.* Proliferative effects of 'fibre' on the intestinal epithelium: relationship to gastrin, enteroglucagon and PYY. *Gut* **28**(Suppl): 221–226 (1987).
20. Roos, S. & Jonsson, H. A high-molecular-mass cell-surface protein from Lactobacillus reuteri 1063 adheres to mucus components. *Microbiology* **148,** 433–442 (2002).
21. Donohoe, D. R. *et al.* The microbiome and butyrate regulate energy metabolism and autophagy in the mammalian colon. *Cell Metab.* **13,** 517–526 (2011).
22. Fukuda, S. *et al.* Bifidobacteria can protect from enteropathogenic infection through production of acetate. *Nature* **469,** 543–547 (2011).
23. Okamoto, T. *et al.* Preventive efficacy of butyrate enemas and oral administration of Clostridium butyricum M588 in dextran sodium sulfate-induced colitis in rats. *J. Gastroenterol.* **35,** 341–346 (2000).
24. Scheppach, W. Treatment of distal ulcerative colitis with short-chain fatty acid enemas. A placebo-controlled trial. German-Austrian SCFA Study Group. *Dig. Dis. Sci.* **41,** 2254–2259 (1996).
25. Scheppach, W. *et al.* Effect of butyrate enemas on the colonic mucosa in distal ulcerative colitis. *Gastroenterology* **103,** 51–56 (1992).
26. Sola-Penna, M. Metabolic regulation by lactate. *IUBMB Life* **60,** 605–608 (2008).
27. Gladden, L. B. Lactate metabolism: a new paradigm for the third millennium. *J. Physiol.* **558,** 5–30 (2004).
28. Bordone, L. & Guarente, L. Calorie restriction, SIRT1 and metabolism: understanding longevity. *Nat. Rev. Mol. Cell. Biol.* **6,** 298–305 (2005).
29. Colman, R. J. *et al.* Caloric restriction delays disease onset and mortality in rhesus monkeys. *Science* **325,** 201–204 (2009).
30. Omodei, D. & Fontana, L. Calorie restriction and prevention of age-associated chronic disease. *FEBS Lett.* **585,** 1537–1542 (2011).
31. Date, Y. *et al.* New monitoring approach for metabolic dynamics in microbial ecosystems using stable-isotope-labeling technologies. *J. Biosci. Bioeng.* **110,** 87–93 (2010).
32. Muyzer, G. *et al.* In *Molecular Microbial Ecology Manual* Vol. 3.4.4 (eds Akkermans, A., van Elsas, J. D. & de Bruijin, F., 1998).
33. Yu, Z. & Morrison, M. Comparisons of different hypervariable regions of rrs genes for use in fingerprinting of microbial communities by PCR-denaturing gradient gel electrophoresis. *Appl. Environ. Microbiol.* **70,** 4800–4806 (2004).
34. Nenci, A. *et al.* Epithelial NEMO links innate immunity to chronic intestinal inflammation. *Nature* **446,** 557–561 (2007).
35. Shiomi, Y. *et al.* GCMS-based metabolomic study in mice with colitis induced by dextran sulfate sodium. *Inflamm. Bowel Dis.* **17,** 2261–2274 (2011).
36. Tsugawa, H. *et al.* Practical non-targeted gas chromatography/mass spectrometry-based metabolomics platform for metabolic phenotype analysis. *J. Biosci. Bioeng.* **112,** 292–298 (2011).
37. Fukuda, S. *et al.* Evaluation and characterization of bacterial metabolic dynamics with a novel profiling technique, real-time metabolotyping. *PLoS One* **4,** e4893 (2009).
38. Nakanishi, Y. *et al.* Dynamic omics approach identifies nutrition-mediated microbial interactions. *J. Proteome Res.* **10,** 824–836 (2011).
39. Osawa, E. *et al.* Predominant T Helper Type 2-inflammatory responses promote murine colon cancers. *Int. J. Cancer* **118,** 2232–2236 (2006).

Acknowledgements

This work was supported partly by grants and contracts from the programme Grants-in-Aid for Scientific Research (B) and Grants-in-Aid for Young Scientists (B) from the Ministry of Education, Cultures, Sports, Science, and Technology; Japan Science and Technology Agency; a grant from the National Center for Global Health and Medicine (21-110, 22-205, 21-129), Ministry of Health, Labor, and Welfare; RIKEN RCAI; and Health and Labor Sciences Research Grants for research on intractable diseases from Ministry of Health, Labor and Welfare of Japan; grants for the Global COE Program, Global Center of Excellence for Education and Research on Signal Transduction Medicine in the Coming Generation from the Ministry of Education, Culture, Sports, Science, and Technology of Japan (M. Yoshida); and for the project research (Development of fundamental technology for analysis and evaluation of functional agricultural products and functional foods) from the Ministry of Agriculture, Forestry, and Fisheries of Japan (M. Yoshida). We thank Dr M. Tamura-Nakano in NCGM EM Support Unit for her technical support for histological analysis.

Author contributions

T. D. designed the study, analyzed data and wrote the paper. T. Okada developed the experimental system, performed *in vivo* experiments and analyzed data. S.F., K. Hase and H.O. performed experiments and analyzed data of germ-free and gnotobiotic mice, bacteriological analysis and gene profiling and wrote the paper. S.N, Y.I. and M. Yoshida performed chemical analyses including all metabolome analysis. T.H., R.K., M. Yamazaki, T. Oshio, T. Otusbo, K.K., K.I.-O., K. Higuchi, and Y.I.K. carried out experiments including cell separation and histological experiments and data analysis.

Additional information

Accession codes: microarray data have been deposited in the Gene Expression Omnibus database under accession code GSE40370.

Supplementary Information accompanies this paper at http://www.nature.com/naturecommunications

Competing financial interests: The authors declare no competing financial interests.

Reprints and permission information is available online at http://npg.nature.com/reprintsandpermissions/

How to cite this article: Okada, T. *et al.* Microbiota-derived lactate accelerates colon epithelial cell turnover in starvation-refed mice. *Nat. Commun.* 4:1654 doi: 10.1038/ncomms2668 (2013).